Available online at www.sciencedirect.com
ScienceDirect
International Journal of Hydrogen Energy 32 (2007) 3734–3742
International Journal of HYDROGEN ENERGY
www.elsevier.com/locate/ijhydene

On hydrogen-induced plastic flow localization during void growth and coalescence

D.C. Ahn[a], P. Sofronis[a,*], R.H. Dodds Jr.[b]

[a]*Department of Mechanical Science and Engineering, University of Illinois at Urbana-Champaign, 1206 West Green Street, Urbana, IL 61801, USA*
[b]*Department of Civil and Environmental Engineering, University of Illinois at Urbana-Champaign, 205 North Mathews Avenue, Urbana, IL 61801, USA*

Available online 10 October 2006

Abstract

Hydrogen-enhanced localized plasticity (HELP) is recognized as a viable mechanism of hydrogen embrittlement. A possible way by which the HELP mechanism can bring about macroscopic material failure is through hydrogen-induced accelerated void growth and coalescence. Assuming a periodic array of spherical voids loaded axisymmetrically, we investigate the hydrogen effect on the occurrence of plastic flow localization upon void growth and its dependence on macroscopic stress triaxiality. Under a macroscopic stress triaxiality equal to 1 and prior to void coalescence, the finite element calculation results obtained with material data relevant to A533B steel indicate that a hydrogen-induced localized shear band forms at an angle of about 45° from the axis of symmetry. At triaxiality equal to 3, void coalescence takes place by accelerated hydrogen-induced localization of plasticity mainly in the ligament between the voids. Lastly, we discuss the numerical results within the context of experimental observations on void growth and coalescence in the presence of hydrogen.

Keywords: Hydrogen; Embrittlement; Void growth; Coalescence; Plasticity

1. Introduction

It is well known that hydrogen-enhanced localized plasticity (HELP) is a mechanism for hydrogen embrittlement whereby hydrogen promotes macroscopic material failure through localized deformation processes [1,2]. The objective of this work is to investigate the hydrogen effect on plastic flow localization during void growth and coalescence as a function of the hydrostatic constraint, that is, low and high stress triaxiality prevalent in cylindrical bar specimens strained uniaxially and ahead of blunting crack tips, respectively. The study is important toward understanding the conditions under which the HELP mechanism promotes ductile crack propagation at load levels that a hydrogen-free material can safely sustain.

There exists ample experimental evidence that hydrogen affects void growth and coalescence. Performing three-point bending tests on U-notched bend bars of spheroidized AISI 1095 and AISI 1090 steels, Hirth and co-workers [3,4] found that hydrogen reduces the critical strain for void nucleation and increases the population of voids. They suggested that hydrogen by enhancing void nucleation and growth promotes plastic instability along characteristic slip traces beneath the notch. Cialone and Asaro [5] using smooth and notched tensile specimens of spheroidized plain-carbon steels found that hydrogen assists void growth and accelerates void coalescence [6]. Garber et al. [7,8] carried out tensile experiments using cylindrical specimens of 1018 and 1080 steels. While they did not observe a significant hydrogen effect on void growth at the initial stages of growth, they found a strong effect during the coalescence stage. Park and Thompson [9] also observed a similar effect in 1520 steel and Fan and Koss [10] in low carbon steels. Maier et al. [11] studied the hydrogen effect on void behavior in a spheroidized low alloy steel using smooth unnotched tensile specimens. They observed that hydrogen enhances void nucleation and promotes final brittle failure by plastic shear localization.

Liang et al. [12] simulated void growth and coalescence in the presence of hydrogen in a niobium system under the assumption that hydrogen is in equilibrium with local stress in

* Corresponding author. Tel.: +1 217 333 2636; fax: +1 217 244 5707.
E-mail address: sofronis@uiuc.edu (P. Sofronis).

0360-3199/$ - see front matter © 2006 International Association for Hydrogen Energy. Published by Elsevier Ltd. All rights reserved.
doi:10.1016/j.ijhydene.2006.08.047

the matrix around a void. Their finite element calculation results support the argument that while hydrogen has a negligible effect on void growth at the early stages of straining, it does accelerate the coalescence stage. The underlying mechanism by which hydrogen was found to promote void coalescence is localized material softening that varied point-wise in the matrix depending on the corresponding hydrogen distribution around the void. In fact, Liang et al. found out that at the final stages of growth hydrogen promotes the localization of plasticity in the ligament between voids which leads to final void coalescence. We note that Liang et al. found that such localization of plasticity during the coalescence stage is the case at all levels of triaxiality, even in the absence of hydrogen. They identified the role of hydrogen in the triggering of the localization process at lower macroscopic strains than in the absence of hydrogen.

In the present study, we analyze the hydrogen effect on void growth and coalescence using material data pertinent to the nuclear reactor steel A533B. Unlike the niobium system used in the investigation of Liang et al. [12], A533B steel is an iron system that can trap hydrogen in vast amounts as deformation proceeds [13–15]. Trapping of hydrogen can drastically affect the material constitution and this can have a significant effect on the conditions for plastic flow localization even at small triaxialities. It will be shown that at small triaxialities and before void coalescence the presence of strong hydrogen trapping leads to the formation of a localized band at an angle of about 45° from the direction defined by the intervoid-ligaments.

Following Liang et al. [12] we simulate the hydrogen effect on void growth and coalescence at a unit cell containing a spherical void and loaded remotely by principal axisymmetric stresses. Results obtained under various levels of applied stress triaxiality can be viewed as representing the behavior of a void at different locations in the neighborhood of a blunting crack tip (Fig. 1).

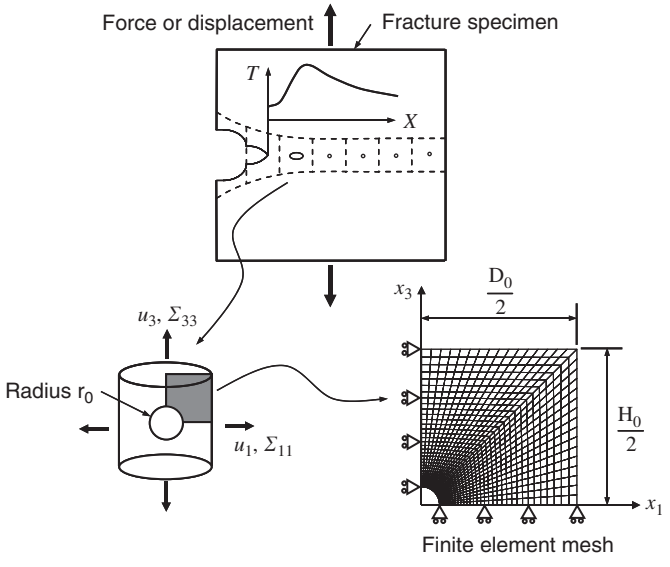

Fig. 1. The axisymmetric unit cell model and the finite element mesh for the first quadrant. The cell is strained while the triaxiality $T = (2\Sigma_{11} + \Sigma_{33})/3|\Sigma_{33} - \Sigma_{11}|$ is maintained constant.

2. Hydrogen concentration and constitutive law

Hydrogen dissolved in metals and alloys resides either at normal interstitial lattice sites (NILS) or reversible trapping sites at microstructural defects generated by plastic straining such as dislocations. The two populations are assumed to be in equilibrium according to Oriani's theory [16] such that

$$\frac{\theta_T}{1-\theta_T} = \frac{\theta_L}{1-\theta_L}\exp\left(\frac{W_B}{R\Theta}\right), \tag{1}$$

where θ_L denotes the occupancy of the interstitial sites, θ_T denotes the occupancy of the trapping sites, W_B is the trap binding energy, R is the gas constant equal to $8.31\,\mathrm{j\,mol^{-1}\,K^{-1}}$, and Θ is the absolute temperature. The hydrogen concentration at trapping sites C_T, measured in hydrogen atoms per unit volume, can be expressed as $C_T = \theta_T \alpha N_T$, where α denotes the number of sites per trap, and $N_T = N_T(\varepsilon^p)$ denotes the trap density in traps per unit volume as a function of the local plastic straining measured in terms of the effective plastic strain ε^p. The hydrogen concentration C_L at NILS, measured in hydrogen atoms per unit volume, can be phrased as $C_L = \theta_L \beta N_L$, where β denotes the number of NILS per solvent atom, and N_L denotes the number of solvent atoms per unit volume given by $N_L = N_A/V_M$ in which $N_A = 6.0232 \times 10^{23}$ atoms per mole is Avogadro's number and V_M is the molar volume of the host lattice.

Using Fermi–Dirac statistics [17], we calculate the hydrogen concentration C_L in terms of the NILS concentration C_L^0 in the stress-free lattice by assuming equilibrium with local stress $\boldsymbol{\sigma}$:

$$\frac{\theta_L}{1-\theta_L} = \frac{\theta_L^0}{1-\theta_L^0}\exp\left(\frac{\sigma_{kk}V_H}{3R\Theta}\right), \tag{2}$$

where $\theta_L^0 = C_L^0/\beta N_L$ is the initial occupancy of NILS, σ_{kk} is the local hydrostatic stress, V_H is the partial molar volume of hydrogen in solution, and a repeated index implies standard summation convention. Occupancy θ_L is a function of the hydrostatic stress as regions under tension attract hydrogen solutes [13,17].

Combining Eqs. (1) and (2), we find the total hydrogen concentration $c = (C_L + C_T)/N_L$, measured in hydrogen atoms per solvent atom, as a function of both the hydrostatic stress and the equivalent plastic strain as

$$c = c_L + c_T = \beta\left[\theta_L(\sigma_{kk}) + \frac{\alpha}{\beta}\frac{N_T(\varepsilon^p)}{N_L}\theta_T\right], \tag{3}$$

where $c_L = C_L/N_L$ and $c_T = C_T/N_L$. Eq. (3) defines the total hydrogen concentration at a point as a function of the effective plastic strain ε^p and hydrostatic stress σ_{kk}.

Based on experimental observations of hydrogen-induced dislocation velocity enhancement in iron, Tabata and Birnbaum [18] suggested that the local flow stress of the material is a decreasing function of the hydrogen concentration. Sofronis et al.

[19] and Liang et al. [20] described the hydrogen effect on the local flow stress σ_Y through a phenomenological relation,

$$\sigma_Y(\varepsilon^p, c) = \sigma_0(c)\left(1 + \frac{\varepsilon^p}{\varepsilon_0}\right)^N, \tag{4}$$

in which c is the total hydrogen concentration in trapping sites and NILS measured in hydrogen atoms per solvent atom, N is the hardening exponent, $\sigma_0(c)$ is the initial yield stress in the presence of hydrogen, $\sigma_0 = \sigma_0(0)$ is the initial yield stress in the absence of hydrogen, and $\varepsilon_0 = \sigma_0/E$ is the corresponding yield strain with E being Young's modulus. A possible suggestion for $\sigma_0(c)$ is

$$\sigma_0(c) = \begin{cases} \left[(\xi - 1)\frac{c}{c_L^0} + 1\right]\sigma_0 & \text{for } \sigma_0(c) > \eta\sigma_0, \\ \eta\sigma_0 & \text{for } \sigma_0(c) \leqslant \eta\sigma_0, \end{cases} \tag{5}$$

where $\xi \leqslant 1$ is a softening parameter, $\eta\sigma_0$ is the lowest value of the yield stress with η varying between 0 and 1, and c_L^0 is the initial hydrogen concentration in the unstressed lattice measured in hydrogen atoms per solvent atom.

For the elastoplastic constitutive law of the material in the presence of hydrogen, we assume that the total deformation rate tensor $\mathbf{D}$—the symmetric part of the velocity gradient—is the sum of an elastic part $\mathbf{D}^e$, a plastic part $\mathbf{D}^p$, and a part due to the presence of hydrogen $\mathbf{D}^h$:

$$\mathbf{D} = \mathbf{D}^e + \mathbf{D}^p + \mathbf{D}^h. \tag{6}$$

We assume that the elastic behavior of the material is linear and isotropic:

$$\mathbf{D}^e = \mathbf{C}^{e-1} : \overset{\nabla}{\boldsymbol{\sigma}} = \left(\frac{1}{2\mu}\mathbf{K} + \frac{1}{3K}\mathbf{J}\right) : \overset{\nabla}{\boldsymbol{\sigma}}, \tag{7}$$

where $\mathbf{C}^e$ is the fourth order tensor of the elastic moduli, $\mathbf{K} = \mathbf{I} - \mathbf{J}$ is the deviatoric part of the fourth order identity tensor $\mathbf{I}$ whose Cartesian components are $I_{ijkl} = (\delta_{ik}\delta_{jl} + \delta_{jk}\delta_{il})/2$ with δ_{ij} being the Kronecker delta, $\mathbf{J} = \boldsymbol{\delta}\,\boldsymbol{\delta}/3$ is the hydrostatic part of the identity tensor $\mathbf{I}$, $\boldsymbol{\delta}$ is the second order identity tensor, $\boldsymbol{\sigma}$ is the Cauchy stress, μ and K are, respectively, the shear and bulk moduli, a superposed ∇ denotes the Jaumann rate, the superscript -1 denotes tensor inverse, and $\mathbf{A} : \mathbf{B} = A_{ijkl}B_{kl}$, where $\mathbf{A}$ and $\mathbf{B}$ are, respectively, fourth and second order tensors.

We write the rate of dilatational [21] deformation $\mathbf{D}^h$ due to dissolved hydrogen as

$$\mathbf{D}^h = \frac{d}{dt}\left[\ln\left(1 + \frac{1}{3}(c - c_0)\frac{\Delta v}{\Omega}\right)\right]\boldsymbol{\delta} = \frac{1}{3}A(c)\dot{c}\,\boldsymbol{\delta}, \tag{8}$$

where the parameter c_0 is the initial hydrogen concentration in NILS and trapping sites measured in hydrogen atoms per solvent atom, $\Delta v = V_H/N_A$ is the volume dilatation per atom of hydrogen introduced into solution, V_H the partial molar volume of hydrogen in solution, Ω the mean atomic volume of the host atom, and a superposed dot denotes material time derivative. For the plastic behavior, we assume that the material is rate independent, obeys von-Mises yielding, and hardens isotropically under plastic straining. The yield criterion is of the form

$$f = \sigma_e - \sigma_Y(\varepsilon^p, c), \tag{9}$$

where $\sigma_e = \sqrt{3\boldsymbol{\sigma}' : \boldsymbol{\sigma}'/2}$ is the von-Mises equivalent stress, $\boldsymbol{\sigma}'$ is the deviatoric part of the Cauchy stress defined through $\boldsymbol{\sigma}' = \mathbf{K} : \boldsymbol{\sigma}$, and $\varepsilon^p = \int \sqrt{2\mathbf{D}^p : \mathbf{D}^p/3}\,dt$ is the effective plastic strain. Assuming normality for the derivation of the flow rule for $\mathbf{D}^p$ and using Eqs. (7)–(9), we derive the constitutive law accounting for hydrogen-induced material softening and lattice dilatation:

$$\overset{\nabla}{\boldsymbol{\sigma}} = \left(\mathbf{C}^e - \frac{9\mu^2}{h + 3\mu}\frac{\boldsymbol{\sigma}'\boldsymbol{\sigma}'}{\sigma_e^2}\right) : (\mathbf{D} - \mathbf{D}^h) + \frac{3\mu}{h + 3\mu}\frac{\partial\sigma_Y}{\partial c}\dot{c}\frac{\boldsymbol{\sigma}'}{\sigma_e}, \tag{10}$$

where $h = \partial\sigma_Y/\partial\varepsilon^p$. Eqs. (1)–(10) show that the problem of determining the hydrogen concentration, stress, and plastic strain fields is fully coupled.

3. Unit cell

We model the behavior of an axisymmetric unit cell containing a spherical void [12,22] as shown in Fig. 1. The cell is loaded macroscopically by principal axisymmetric stresses Σ_{11} and Σ_{33} while the stress triaxiality $T = (2\Sigma_{11} + \Sigma_{33})/3|\Sigma_{33} - \Sigma_{11}|$ measuring the ratio of the hydrostatic stress over the deviatoric stress is forced to remain constant during deformation through a Newton iteration scheme [12]. We investigate the behavior of the cell at triaxialities varying from 1 to 3. Such levels of triaxiality are representative of the hydrostatic constraint in uniaxial tension specimens and in the neighborhood of a blunting crack tip. The diameter and height of the unit cell in the undeformed state are D_0 and H_0, respectively. The outer surfaces of the cell are free of shear traction and are forced to remain straight during deformation; the cell remains always axisymmetric with a diameter D and a height H. The macroscopic strains in response to the applied stresses are $E_{11} = \ln(D/D_0)$ and $E_{33} = \ln(H/H_0)$, and the macroscopic effective strain is $E_e = |E_{33} - E_{11}|$. We solve the boundary value problem for the calculation of the hydrogen, stress, and deformation fields in the matrix surrounding the void numerically by using the general purpose finite element program ABAQUS with a "user subroutine" (UMAT) incorporating the material model described in Section 2. Due to symmetry, we analyze only the first quadrant of the unit cell (Fig. 1).

4. Numerical results

We used material data relevant to the A533B nuclear reactor pressure vessel steel: $\sigma_0 = 400$ MPa, Young's modulus $E = 200$ GPa, Poisson's ratio $\nu = 0.3$, and hardening exponent $N = 0.1$. The molar volume of iron is 7.116×10^{-6} m^3/mol and therefore $N_L = 8.46 \times 10^{28}$ solvent lattice atoms/m^3. The hydrogen partial molar volume in solution is 2.0×10^{-6} m^3/mol. The parameters α and β used in the definitions of the trapping and NILS concentrations were both taken equal to 1. We assumed the trap density N_T to increase with plastic straining ε^p according to the experimental results of Kumnick and Johnson [23] and we obtained the function $N_T(\varepsilon^p)$ by interpolating

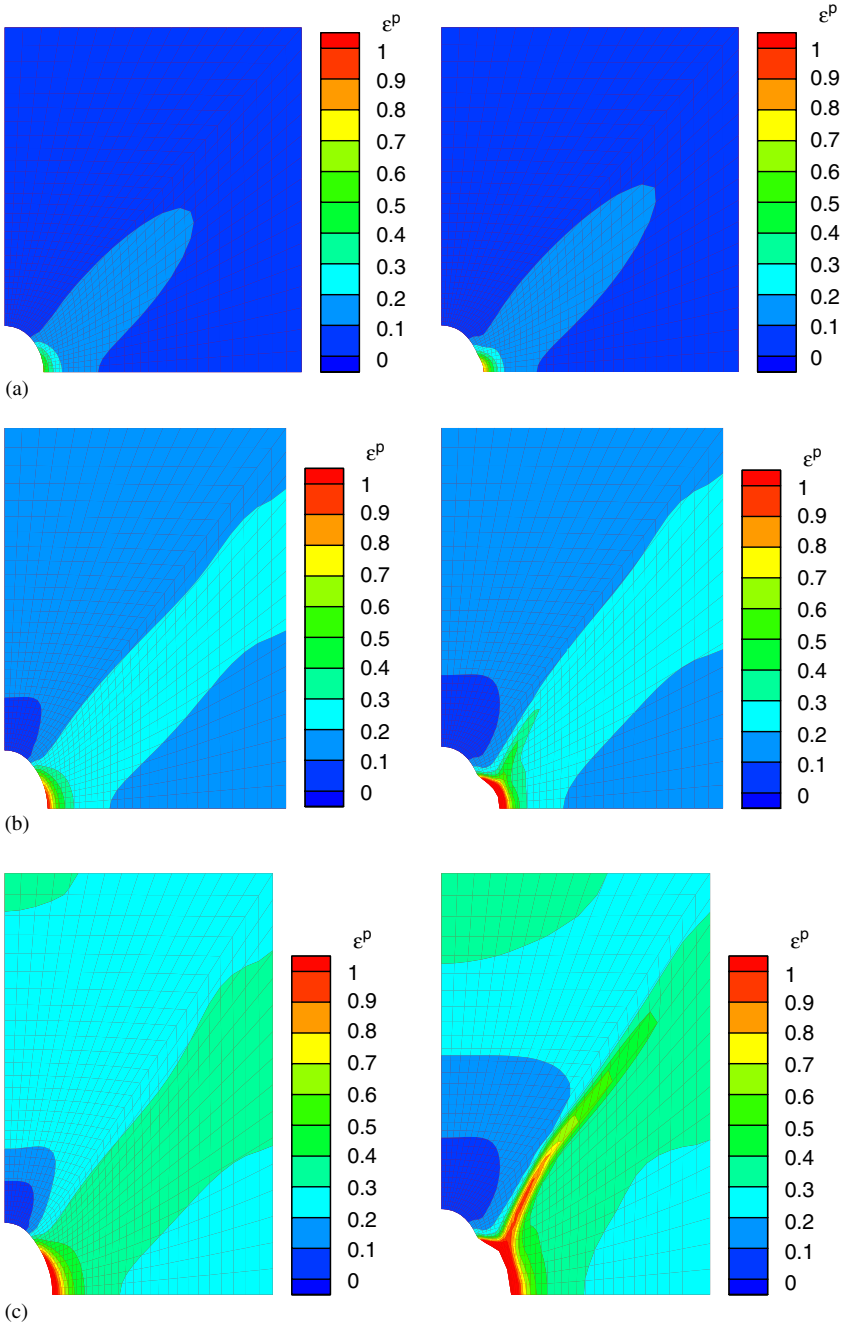

Fig. 2. Local effective plastic strain distribution at stress triaxiality $T = 1$ and various levels of macroscopic effective strain $E_e = |E_{33} - E_{11}|$. The left column is for the hydrogen-free material and the right column is for the material at an initial NILS concentration of 2.4634×10^{-8} hydrogen atoms per solvent atom. The void volume fraction before deformation is 0.001. (a) Macroscopic effective strain $E_e = 0.1$; (b) macroscopic effective strain $E_e = 0.2$; (c) macroscopic effective strain $E_e = 0.3$.

the experimental data. We set the trap binding energy equal to 60 kJ/mol [23]. For the softening parameters ξ and η, we assumed to be equal to 0.99 and 0.5, respectively. A 0.99 value for ξ is associated with 1% reduction of the initial yield stress at the initial concentration of hydrogen c_L^0 in NILS before the application of the load, and a 0.5 value for η denotes a maximum allowed reduction of 50% in the initial yield stress at all stages of straining. For the stress-free lattice, we assumed a uniform hydrogen concentration $C_L^0 = 2.084 \times 10^{21}$ atoms/m^3 ($c_L^0 = 2.4634 \times 10^{-8}$ atoms per solvent atom) throughout in equilibrium with gas at 1 atm pressure. The unit cell dimensions D_0 and H_0 were both equal to 200 μm, the initial void volume fraction was $f_0 = 0.001$, and the temperature of the system 300 K.

Figs. 2 and 3 show the effective plastic strain distribution at the unit cell both in the absence of hydrogen (left column) and

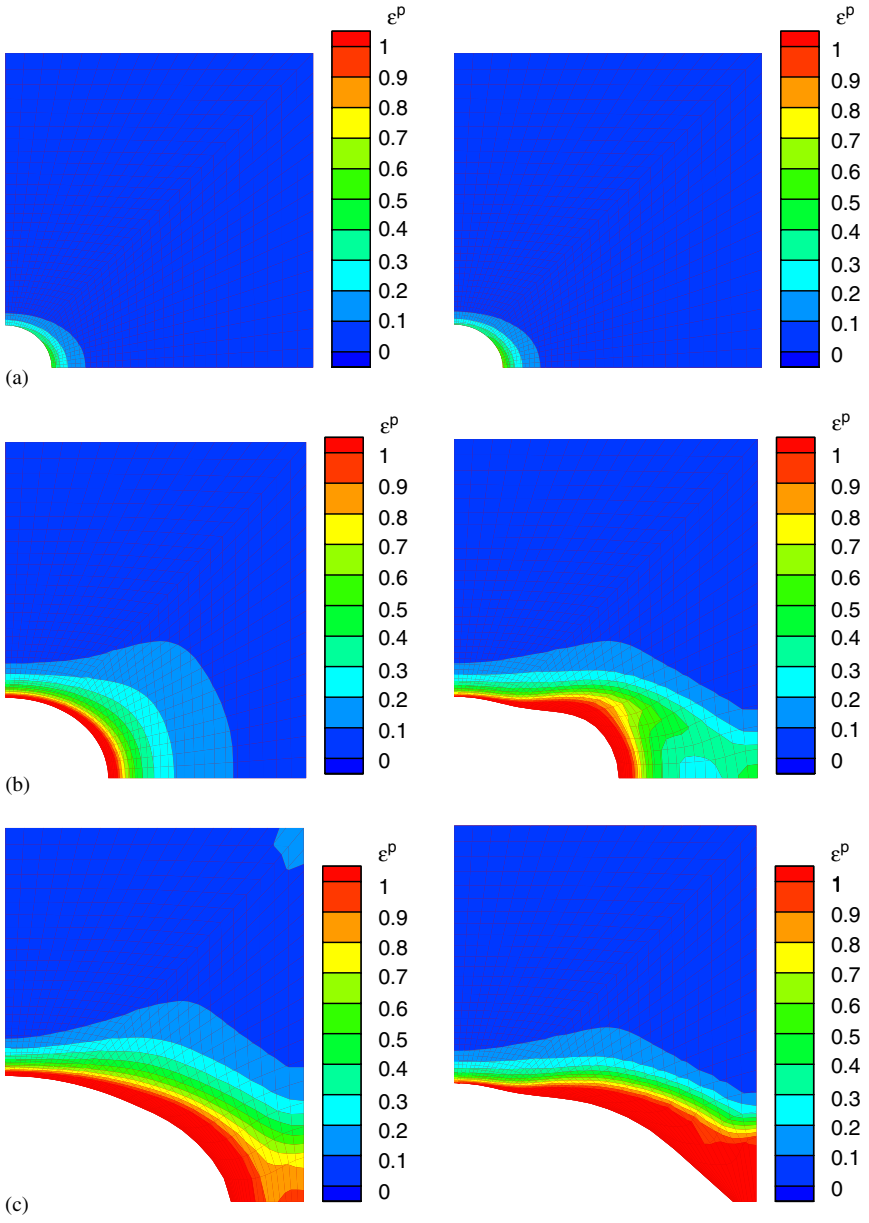

Fig. 3. Local effective plastic strain distribution at stress triaxiality $T = 3$ and various levels of macroscopic effective strain E_e. The left column is for the hydrogen-free material and the right column is for the material at an initial NILS concentration of 2.4634×10^{-8} hydrogen atoms per solvent atom. The void volume fraction before deformation is 0.001. (a) Macroscopic effective strain $E_e = 0.015$; (b) macroscopic effective strain $E_e = 0.075$; (c) macroscopic effective strain $E_e = 0.15$.

in the presence of hydrogen (right column) when the applied stress triaxiality T equals 1 and 3, respectively. At triaxiality $T = 1$, hydrogen induces a localized shear band initiating at the void surface and propagating toward the interior bulk material. At triaxiality $T = 3$, hydrogen causes the void to grow into an oblate spheroid faster than in the absence of hydrogen. It is interesting that no localized shear deformation is observed at this high triaxiality of 3. Instead, the plastic deformation is confined close to the void surface and in the ligament between the voids. The normalized hydrogen concentrations c_L/c_L^0 at NILS and c_T/c_L^0 at trapping sites are shown in Fig. 4 at triaxiality 1 and in Fig. 5 at triaxiality 3. At $T = 1$ and macroscopic effective strain of 0.3, Fig. 4b shows that hydrogen accumulates preferentially in the narrow shear band in which severe plastic deformation takes place (see Fig. 2c) and close to the void surface in the ligament between the voids. On the other hand, at triaxiality $T = 3$, Fig. 5b shows that hydrogen accumulates in a narrow zone around the deformed void surface. It is clear from Figs. 4 and 5 that hydrogen predominantly resides at traps generated by plastic straining. Fig. 6 shows the distribution of the normalized yield stress $\sigma_0(c)/\sigma_0$ at the unit cell. At triaxiality $T = 1$, localized softening is observed within the shear band location (Fig. 2c) in accordance with the localized hydrogen accumulation (Fig. 4b). In contrast, at triaxiality

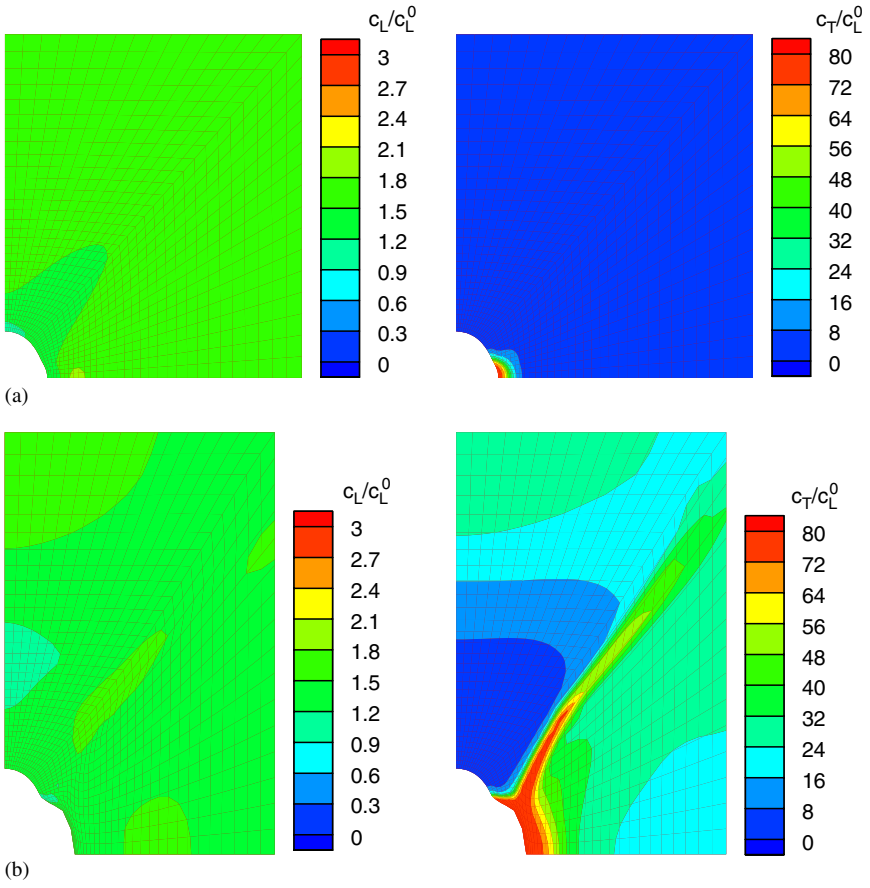

Fig. 4. Distribution of the normalized hydrogen concentration c_L/c_L^0 at NILS (left column) and c_T/c_L^0 at trapping sites (right column) at stress triaxility $T = 1$ and two levels of macroscopic effective strain E_e. (a) Macroscopic effective strain $E_e = 0.1$; (b) macroscopic effective strain $E_e = 0.3$.

$T = 3$, substantial softening is the case around the void and at the ligament between the voids (Figs. 3b and 5b). At both triaxialities, softening is associated with trapped hydrogen. Fig. 7 shows the normalized void volume fraction as a function of the macroscopic effective strain at various levels of triaxiality. Significantly, hydrogen increases the rate of growth as the macroscopic strain increases and reduces the macroscopic strain at which coalescence occurs.

Investigating void growth in a niobium system with a void volume fraction $f_0 = 0.0013$, Liang et al. [12] found almost a negligible hydrogen effect on void growth and coalescence at triaxialities $T = 2$ and 3, but a marked effect at triaxiality $T = 1$ (see their Fig. 3b). Thus, whereas the hydrogen effect on void growth and coalescence in the niobium system is mainly observed at small triaxialities, in iron systems it affects both growth and coalescence at all triaxialities as shown by Fig. 7.

5. Discussion

Figs. 2, 3, and 7 show that as straining increases hydrogen progressively accentuates void growth and accelerates the coalescence stage at all levels of stress triaxialities. In particular, the effect on void coalescence is more pronounced at small triaxialities, e.g. $T = 1$. Since hydrogen solutes in iron and steel accumulate at much larger quantities at trapping sites [14,15] than at NILS, the hydrogen softening effect on void growth and coalescence becomes stronger at larger plastic strains at which hydrogen tends to get trapped at microstructural defects. It is noted that the density of traps, e.g. dislocations, increases with plastic deformation. Indeed, at large macroscopic strains, namely E_e=0.3 under triaxiality T=1 and E_e=0.075 under triaxiality T=3, hydrogen resides predominantly at trapping sites (see Figs. 4b and 5b) in the neighborhood of the void surface.

At high-constraint configurations, e.g., at triaxiality T=3, as in the neighborhood of U-notched bend specimens or notched tensile specimens, the present numerical simulations indicate a strong hydrogen effect on void coalescence [1,2,5]. Fig. 3 shows clearly that as straining increases, hydrogen enhances the void growth rate and accelerates the coalescence stage. It is well known that void growth is strongly dependent on stress triaxiality [22,24,25]. As shown from Figs. 2a and 3b, with both cells strained at macroscopic effective strain $E_e \leqslant 0.1$, the void grows larger at triaxiality $T = 3$ than at $T = 1$ in the absence of hydrogen. Such larger void growth is associated with larger plastic straining, which in the presence of hydrogen brings about larger hydrogen accumulations at trapping sites causing more extensive material softening, which in turn brings

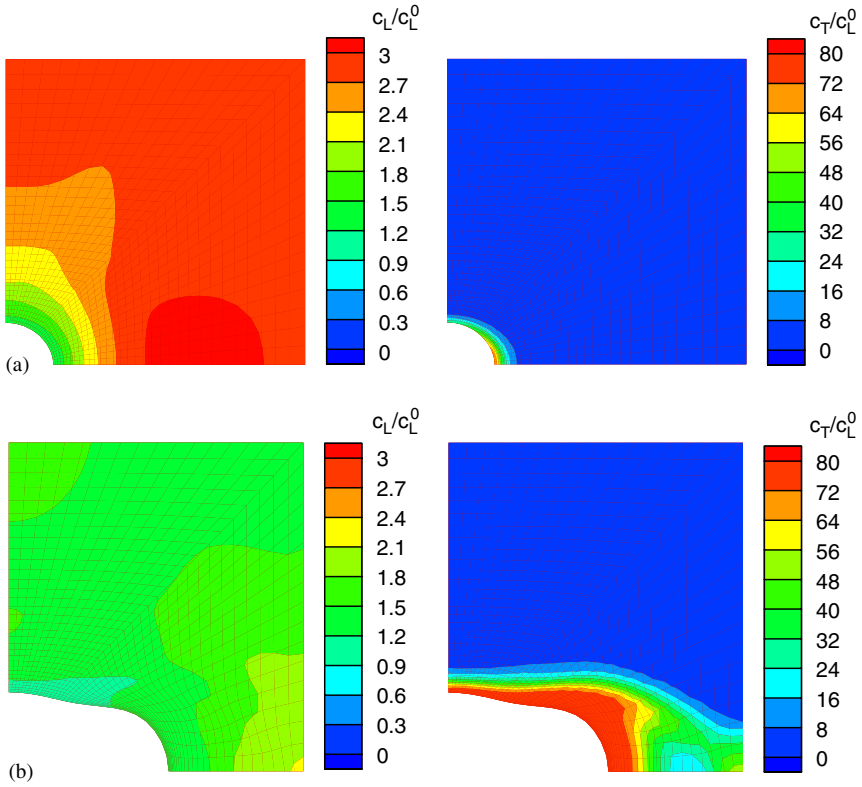

Fig. 5. Distribution of the normalized hydrogen concentration c_L/c_L^0 at NILS (left column) and c_T/c_L^0 at trapping sites (right column) at stress triaxiality $T = 3$ and two levels of macroscopic effective strain E_e. (a) Macroscopic effective strain $E_e = 0.015$; (b) macroscopic effective strain $E_e = 0.075$.

about the coalescence stage at lower macroscopic strains. Thus, at large triaxialities, e.g. $T = 3$, the synergistic effect of triaxiality and hydrogen-induced softening promotes substantial void growth even at low macroscopic strains ($E_e = 0.075$, see Figs. 3b and 7).

Acceleration of void coalescence has been observed to be the case in the failure of specimens strained in uniaxial tension [5–10]. At triaxiality $T = 1$, Fig. 2c shows that hydrogen-induced material softening causes the deformation around a void to concentrate in a localized shear band emanating from the void surface. No such intense shear band is observed in the absence of hydrogen (Fig. 2c). Thus, if hydrogen-induced failure occurs at low triaxialities, which in uniaxial tension may be the case in the absence of substantial specimen necking, it is facilitated by localized shear bands emanating from the void surfaces at 45°. Park and Thompson [9] observed that hydrogen-assisted ductile fracture in cylindrical specimens of spheroidized 1520 steel is caused by enhanced shear localization in the matrix ligaments between the voids and in the presence of some hydrogen-induced reduction-of-area loss, though not substantial.

At triaxiality $T=1$, hydrogen accumulates inside the band of intense shear emanating from the void surface (Fig. 4b). Notably, the surrounding area is depleted of hydrogen. Further, no similar localized shear band was observed in the simulations of Liang et al. [12] in the niobium system under the same triaxiality of 1. The difference in the plastic response between the two systems at $T = 1$ can be explained by the fact that (i) softening in the work of Liang et al. was characterized by $\eta = 0.9$ whereas $\eta = 0.5$ in the present study. Thus, hydrogen-induced softening is modeled as more intense in the present study than in the work of Liang et al. at the same hydrogen concentration; (ii) softening in niobium is effectively a result of NILS hydrogen whereas softening in iron is a result of trapped hydrogen. In the niobium system, softening tends to be more uniform throughout the matrix as it is the NILS hydrogen that dominates the hydrogen populations. The gradients of NILS populations which follow the hydrostatic stress distribution are not as strong as those of the trapping site concentrations which follow the plastic strain distribution. Moreover, the dominant trapping site populations in the iron systems develop at the void surface—where they initiate localized shear—whereas the dominant NILS populations in the niobium system develop at the center of the inter-void ligament.

Such continued accumulation of hydrogen inside shear bands is a key issue in the HELP mechanism for hydrogen embrittlement. Hydrogen by triggering a localized shear band continues to promote the localization of deformation by continuing to accumulate preferentially in the band. Thus, macroscopic failure can take place easily through localized shear sustained by hydrogen. In agreement with this discussion, Fig. 6 shows that hydrogen-induced material softening when expressed in terms of the reduction in the yield stress follows the corresponding

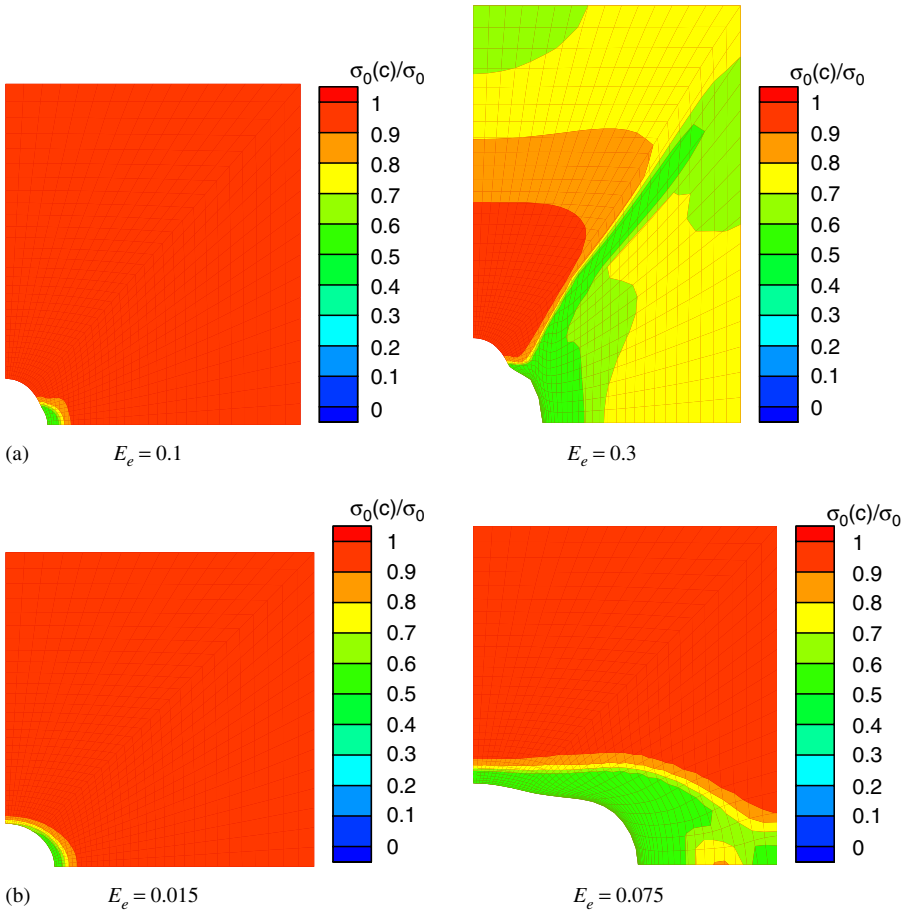

Fig. 6. Distribution of the normalized yield stress $\sigma_0(c)/\sigma_0$ in the presence of hydrogen. The parameter σ_0 denotes the yield stress in the absence of hydrogen. (a) Stress triaxiality $T = 1$; (b) stress triaxiality $T = 3$.

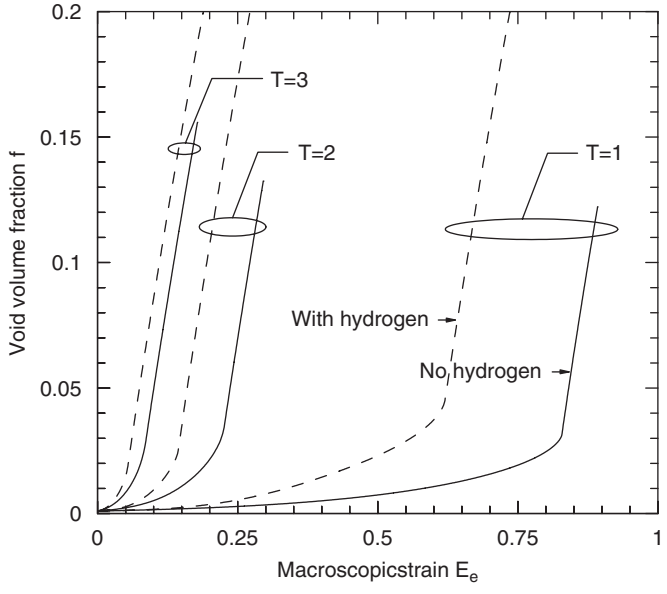

Fig. 7. Plot of the void volume fraction f versus the macroscopic effective strain E_e at various levels of stress triaxiality T. The initial void volume fraction is $f_0 = 0.001$.

hydrogen accumulation at all magnitudes of macroscopic strain and applied stress triaxiality.

6. Conclusion

The effect of hydrogen on void growth and coalescence in A533B nuclear reactor pressure vessel steel has been studied at a unit cell containing a spherical void under axisymmetric stress conditions and while hydrogen is in equilibrium with local hydrostatic stress and plastic strain. Hydrogen was found to promote void growth and coalescence at all levels of triaxiality and applied macroscopic strain. At triaxiality equal to 3, the synergistic effect of high stress triaxiality and hydrogen-induced softening enhances void growth. The effect of hydrogen on void coalescence increases as the triaxiality decreases. Remarkably, at triaxiality equal to 1, the calculations reveal that hydrogen assists in the formation of a localized shear band emanating form the void surface. The present results can be used to investigate the conditions for the onset and propagation of a crack by void growth and coalescence in the presence of hydrogen as shown in Fig. 1. Such a study is the subject of a subsequent investigation.

Acknowledgments

The authors gratefully acknowledge financial support from the NASA Marshall Space Flight Center (Grant NAG 8-1751; Mr. Doug Wells, Technical Monitor), the National Science Foundation (Grant DMR 0302470), and the US DoE (Grant GO15045, Mr. Mark Paster, Technical Monitor).

References

[1] Birnbaum HK, Robertson IM, Sofronis P, Teter D. Mechanisms of hydrogen related fracture—a review. In: Magnin T, editor. Corrosion deformation interactions CDI'96, Second international conference, Nice, France, 1996. Great Britain: The Institute of Materials; 1997. p. 172–95.

[2] Robertson IM. The effect of hydrogen on dislocation motion. Eng Fract Mech 2001;68:671–92.

[3] Lee TD, Goldenberg T, Hirth JP. Effect of hydrogen on fracture of U-notched bend specimens of spheroidized AISI 1095 steel. Metall Trans A 1979;10A:199–208.

[4] Onyewuenyi OA, Hirth JP. Plastic instability in U-notched bend specimens of spheroidized AISI 1090 steel. Metall Trans A 1982;13: 2209–18.

[5] Cialone H, Asaro RJ. The role of hydrogen in the ductile fracture of plain carbon steels. Metall Trans A 1979;10:367–75.

[6] Cialone H, Asaro RJ. Hydrogen assisted fracture of spheroidized plain carbon steels. Metall Trans A 1981;12:1373–87.

[7] Garber R, Bernstein IM, Thompson AW. Effect of hydrogen on ductile fracture of spheroidized steel. Scr Metall 1976;10:341–5.

[8] Garber R, Bernstein IM, Thompson AW. Hydrogen assisted ductile fracture of spheroidized carbon steels. Metall Trans A 1981;12:225–34.

[9] Park IG, Thompson AW. Hydrogen-assisted ductile fracture in spherodized 1520 steel: Part I. Axisymmetric tension. Metall Trans A 1990;21:465–577.

[10] Fan Y, Koss DA. Hydrogen, stress state, and void vs. hole growth in spheroidized plain carbon steels. In: Louthan Jr. MR, McNitt RP, Sisson Jr. RD, editors. Proceedings of the conference on environmental degradation of engineering materials III. Pennsylvania State University Press; 1987. p. 121–32.

[11] Maier HJ, Popp W, Kaesche H. Effects of hydrogen on ductile fracture of a spheroidized low alloy steel. Mat Sci Eng 1995;191:17–26.

[12] Liang Y, Ahn DC, Sofronis P, Dodds Jr. RH, Bammann D. Hydrogen effect on void growth and coalescence in metals and alloys. Mech Mater 2006, under review.

[13] Hirth JP. Effects of hydrogen on the properties of iron and steel. Met Trans A 1980;11:861–90.

[14] Sofronis P, McMeeking RM. Numerical analysis of hydrogen transport near a blunting crack tip. J Mech Phys Solids 1989;37:317–50.

[15] Taha A, Sofronis P. A micromechanics approach to the study of hydrogen transport and embrittlement. Eng Fract Mech 2001;68:803–37.

[16] Oriani RA. The diffusion and trapping of hydrogen in steel. Acta Metall 1970;18:147–57.

[17] Hirth JP, Carnahan B. Hydrogen adsorption at dislocations and crack is Fe. Acta Metall 1978;26:1795–803.

[18] Tabata T, Birnbaum HK. Direct observations of the effect of hydrogen on the behavior of dislocations in iron. Scr Metall 1983;17:947–50.

[19] Sofronis P, Liang Y, Aravas N. Hydrogen induced shear localization of the plastic flow in metals and alloys. Eur J Mech A Solids 2001;20: 857–72.

[20] Liang Y, Sofronis P, Aravas N. On the effect of hydrogen on plastic instabilities in metals. Acta Mater 2003;51:2717–30.

[21] Peisl H. Lattice strains due to hydrogen in metals. In: Alefeld G, Vokl J, editors. Hydrogen in metals I, topics in applied physics, vol. 28. New York: Springer; 1978. p. 53–74.

[22] Pardoen T, Hutchinson JW. An extended model for void growth and coalescence. J Mech Phys Solids 2000;48:2467–512.

[23] Kumnick AJ, Johnson HH. Deep trapping states for hydrogen in deformed iron. Acta Metall 1980;28:33–9.

[24] McClintock FA. A criterion for ductile fracture by the growth of holes. J Mech Phys Solids 1968;35:363–71.

[25] Rice JR, Tracey DM. On the ductile enlargement of voids in triaxial stress fields. J Mech Phys Solids 1969;17:201–17.